



CFD FOR ROTORCRAFT – RECENT PROGRESS AND NEW CHALLENGES WITH THE GOAHEAD CASE

G.N. Barakos*, R. Steijl* and M. Woodgate*

* School of Engineering - The University of Liverpool, Liverpool L69 3GH, UK

Keywords: *CFD, helicopter*

Abstract

Interactional effects between the main rotor and the fuselage of a helicopter are important for the performance analysis of helicopters especially near the edges of the helicopter flying envelope. Computational Fluid Dynamics is also capable of quantifying these effects although a substantial computational cost. At the same time, assessment and validation of the CFD predictions depend on the availability of experimental data of substantial resolution and quality. The GOAHEAD project, of the 6th European Funding framework, provided valuable wind tunnel measurements for a helicopter model of a relatively complex configuration. Main and tail rotors were present. The wind tunnel investigations included an extensive set of conditions from cruise at high speed, to very high speed flight as well as high disk loading cases. The Helicopter Multi Block solver (HMB) of Liverpool University was the only in-house code from the UK to be used in this project. To account for the relative motion of rotor(s) and fuselage, the sliding plane approach was used. As a first step of the project, a family of multi-block CFD meshes was developed at Liverpool designed to work with the sliding-plane method. For the blind test phase, the tail rotor was omitted. A more advanced multi-block topology was then developed for the post-wind tunnel test phase of the project, which allowed main and tail rotors to be included. These new sets of results were in better agreement with measurements and were also performed on finer meshes. The quality of the CFD mesh is crucial for accurate predictions and an educated guess of the flow regions where severe interactions of flow

structures will occur is of importance for such complex CFD computations. On the other hand, the efficiency of the CFD solver was high, and CFD analyses on meshes of up to 30 million cells were performed during this project. It appears that, overall, the computational framework in HMB is adequate for the estimation of the loads on the components of the helicopter configuration and the flow interactions between the main rotor and the fuselage. The need for trim data, blade structural properties or direct measurements of the blade deformation shows that these areas require further investigation. In particular, the results were sensitive to the employed trim state and although the model blades employed for the test were relatively stiff, knowledge of their exact shape during flight is important for accurate predictions.

1 Introduction

Computational Fluid Dynamics methods have been increasingly used in the design and analysis of rotorcraft. This trend was made possible by the progress in CFD algorithms and the availability of ever more powerful affordable computers. For hovering rotors, often simulated as a steady-state problem for a single blade, the computational overhead has been reduced sufficiently to enable the routine use in the design process of helicopter main and tail rotors. However, the aero-mechanics of an isolated rotor is still a very challenging area, since it constitutes a complex multi-disciplinary problem involving complex vortical wake flows, transonic flow regions, rotor blade dynamics and blade elastic deformation. In the

aeromechanics of a full helicopter configuration, the additional flow physics introduced by the aerodynamic interactions between the main rotor, tail rotor and fuselage have to be considered. Regardless of its importance, interactional helicopter aerodynamics has so far been considered by very few researchers, mainly as a result of the complexities mentioned above [1–7]. In addition to the complex flow physics, the geometric complexity of a full helicopter configuration introduces significant challenges to wind tunnel experiments, as well as, CFD investigations. Therefore, most of the published works concern wind tunnel experiments with generic helicopter rotors mounted on idealized fuselages, e.g. the rotor-cylinder test case of the Georgia Institute of Technology [8, 9] and the ROBIN test case at NASA [10–12].

The present state-of-the-art in CFD investigations of full helicopter configuration has not yet reached the maturity of numerical investigations of hovering rotors or isolated rotors in forward flight. A major factor has been the lack of adequate wind tunnel flight test data for validation purposes. Therefore, an urgent need exists for a database of high quality experimental data, which can act as validation for the state-of-the-art CFD methods.

To address this need, the European Commission funded the Framework 6 Program GOAHEAD, with the aim to create such an experimental data base and to validate state-of-the-art CFD methods. The GOAHEAD experiment was built around a development wind tunnel model of the NH90 aircraft [13].

Regardless of the challenging geometry to model with CFD (Figure 1) and the necessity to resolve several interactions, calculations for this case were performed by several partners across Europe. The Helicopter Multi Block solver (HMB) of Liverpool University [5, 6, 14] was the only in-house code from the UK to be used in this project. To account for the relative motion of rotor(s) and fuselage, the sliding plane approach was used, as detailed previously in Res. [6, 7], and described briefly in Section 2. The CFD grids available to the GOAHEAD partners were designed to work with an over-set grid or CHIMERA approach, since this was the

approach most commonly used by the CFD research groups involved.

2 The HMB Flow Solver

The Helicopter Multi-Block (HMB) CFD code [5,6,14] was employed for this work. HMB solves the unsteady Reynolds-averaged Navier-Stokes equations on block-structured grids using a cell-centred finite-volume method for spatial discretization. Implicit time integration is employed, and the resulting linear systems of equations are solved using a pre-conditioned Generalized Conjugate Gradient method. For unsteady simulations, an implicit dual-time stepping method is used, based on Jameson’s pseudo-time integration approach [15]. The method has been validated for a wide range of aerospace applications and has demonstrated good accuracy and efficiency for very demanding flows. A detailed account of application to dynamic stall problems can be found in Ref. [16]. Several rotor trimming methods are available in HMB along with a blade-actuation algorithm that allows for the near-blade grid quality to be maintained on deforming meshes [14].

The HMB solver has a library of turbulence closures which includes several one- and two- equation turbulence models and even non-Boussinesq versions of the $k - \omega$ model. Turbulence simulation is also possible using either the Large-Eddy or the Detached-Eddy approach. The solver was designed with parallel execution in mind and the MPI library along with a load-balancing algorithm are used to this end. For multi-block grid generation, the ICEM-CFD Hexa commercial meshing tool is used and CFD grids with 10-30 million points and thousands of blocks are commonly used with the HMB solver.

The underlying ideas behind the sliding-mesh approach, as well as the details of the implementation in HMB were previously described in Refs. [6, 7]. The method can deal with an arbitrary number of sliding planes between meshes in relative motion. The main requirement is that the grid boundary surfaces of two meshes on either side of a sliding plane match exactly, while the mesh topology and

meshes can be, and in general are, non-matching. For the computations of the GOAHEAD project the method had to be tested and validated for multiple sliding interfaces that were used to allow for the relative motion of the main and tail rotors with respect to the fuselage. The task of accounting for the data to be exchanged between various processors and the correct interpolation across the sliding meshes was carried out without any substantial penalty in the performance of the solver.

2.1 Computational grid

The GOAHEAD geometry comprises a wind-tunnel model of the NH90 with the 4-bladed ONERA 7AD main rotor, equipped with anhedral tips and parabolic taper, and the BO105 2-bladed tail rotor.

The pre-test phase CFD geometry was based on the CAD model originally used to produce the wind tunnel model. The wind tunnel support was an approximation of the support planned for the test. The model actually tested had a more streamlined wind tunnel support. Also, the fuselage geometry was different from the original CAD model in a number of ways. In our computations the fuselage geometry was left unchanged, with the exception of the correction of the horizontal tail plane anhedral. The mesh parameters for the different grids used in the project are listed in Table 1. The grids generated for the project were designed for Reynolds-Averaged Navier-Stokes simulations without the use of wall-functions, i.e. sufficient near-wall resolution was required to ensure an adequate resolution of the boundary layers.

The rotor meshes employed during the GOAHEAD project were built on a C-H type multi-block topology, where the H-type topology in the span-wise direction takes into account the blade root and tip by incorporating 4 prism-shaped blocks emanating from both ends of the blade. The meshes have a C-type topology in the chord-wise direction, with a good spatial resolution of both leading-edge and trailing-edge of the blades. More details of this type of multi-block meshes for rotors can be

found in Refs. [14]. At first, the tail rotor was omitted from the geometry. This allowed the use of a single sliding-plane surface separating the fuselage mesh and the main rotor mesh. This plane was constructed to be normal to the rotor shaft. Naturally, this single sliding plane required the use of a cylindrical 'far-field' boundary condition. For the post-test phase a more advanced multi-block topology was therefore developed which enabled both main and tail rotors to be included. A significant change relative to the pre-test fuselage topology was the use of the concept of embedding local O-type sub-topologies into the topology for the post-test phase. As before, the topology has a 1-to-1 block face connectivity throughout, which naturally leads to the large number of blocks in the employed topologies. An interesting observation when comparing the topology of the surface meshes for pre-test and post-test phases is that the use of the embedded local O-type sub-topologies results in a reduced complexity of the surface topology and, for the particular grids compared here, a more even distribution of the mesh points with less pronounced localized refinements, as compared to the pre-test topology. The multi-block topology for the post-WT phase of the project was developed before the actual wind-tunnel model geometry was obtained. Therefore, an intermediate family of meshes was developed, i.e. using the multi-block topology for the post-test phase and the CFD geometry from the pre-test phase, excluding the wind tunnel support. For the post-WT meshes, the only change was the addition of the new wind-tunnel support as well as the modification of the horizontal tail plane anhedral angle. Figures 1, 2 and 3 show the geometry and the multi-block structured mesh for the intermediate and post-test phases of the project. For this full helicopter-test phase, the actual wind tunnel support was represented correctly. Both main and tail rotors are placed within a drum-shaped sliding-plane interface, as shown in Figure 1. The close proximity of the main and tail rotor planes is notable in the figure, which leads to an additional challenge in the generation of the multi-block structured meshes used here. The main rotor drum has the 5° forward tilt of the main rotor shaft, while the

tail rotor drum is tilted about the x-axis as well as the z-axis (in the tail rotor hub-centred coordinate system) to provide a small forward and upward tail rotor thrust component.

3 Results and Discussion

The case considered corresponds to an economic cruise condition, for which the free-stream Mach number is 0.204 and the tip Mach number of the rotor 0.62. A representative rotor trim schedule is used in the simulation, i.e. the rotor has cyclic pitch change as well as a harmonic blade flapping. The multi-block topology of the rotors is designed to handle the grid deformation as discussed in Ref. [14].

3.1 Interactional Aerodynamics

Figure 4(a) shows the instantaneous surface pressure distribution at main rotor azimuth 90° of the third revolution for the economic cruise condition at $\mu = 0.3$. The effect of the blade passing on the surface pressure distribution of the front part of the fuselage is shown in detail in Figure 4(b), where $x = 0.75$ plane is shown. The main rotor blade passing through the front of the rotor disk clearly induces a (delayed) pressure rise on the forward fuselage, as discussed previously in Ref. [6]. The interaction of the tail rotor with the fin is shown in Figure 4(c), showing the C_p contours in the $z = 0.775$ cross section. The tail rotor blade is at $\psi = 0^\circ$, which corresponds to the downward vertical position. For the rotation direction of the tail rotor used here, this position is in the retreating side of the tail rotor disk. The blade stagnation pressure in the selected cross-section is therefore only around twice the fin stagnation pressure. In addition to the direct impulsive effect, the tail rotor-fin interaction also includes the effect of the tail rotor induced velocity on the flow around the side-force generating fin, by effectively changing the flow angle in a time-periodic fashion. This effect is more difficult to analyze than the pressure impulse effect show in the figure.

A comparison of simulation results with and without tail rotor would clearly show this contribution. The main rotor-fuselage

interactional effect on the rotor loads for the GOAHEAD model was investigated in detail Ref. [7]. As a first step, the flow around the full helicopter was computed using the 'intermediate' mesh, i.e. the WT-support and the anhedral of the horizontal tail plane were omitted. Then, the main rotor mesh of this grid was embedded in a new background mesh for which the far-field boundaries coincided with the wind tunnel walls, but did not contain the fuselage. Using the sliding-plane approach, the rotor-wind tunnel system was computed with identical computational parameters such as time steps and dual-time step truncation criteria as the previously computed full helicopter case.

For both cases, the blade sectional loading as function of the sectional span-wise position and blade azimuth was extracted. Figure 5 shows an example of the comparison for the blade at the fore and aft positions. Sectional blade loading are compared for the full helicopter and the equivalent isolated rotor case. The results were discussed in more detail in Ref. [7], highlighting the capability of the present sliding plane approach to quantify the effect of the rotor-fuselage interaction. The results clearly showed the extent of the blade inboard stations which were affected by the presence of the fuselage. It was found that the interactional effect is mostly restricted to the front and rear of the disk, i.e. the advancing and retreating sides loading did not change significantly due to the presence of the helicopter fuselage. Secondly, the fuselage induces an up-wash, which effectively increases the blade angle of attack through a significant area at the front of the rotor disk. In a similar vein, the fuselage creates downwash behind the fairing, which leads to a reduction of the blade angle of attack for parts of the rear of the rotor disk. Compared to the up-wash area at the front of the disk, the extent of the downwash area at the rear of the disk appears to be smaller. In particular, at the front of the rotor disk, the interactional effect extends to blade stations further outboard, as compared to the interaction at the rear of the rotor disk.

3.2 Comparisons with experiments

Figures 6 and 7 present the comparison between the unsteady pressure transducers on the GOAHEAD model fuselage and the HMB results for the economic cruise case. On the model surface, coloured spheres are placed near each transducer, with the colour representing the value of the surface pressure coefficient. With minor exceptions of a couple of transducers on the front of the fuselage and on the side of the engine housing, all transducers agree remarkably well with the HMB predictions.

Results are shown for four azimuth angles suggesting that the method is capable of capturing at least the main pressure transients. It is important to highlight here the key role of the experiments and the need to process the experimental data the same way as the CFD results. For Figures 6 and 7, the GOAHEAD data were averaged in phase and with the same resolution as the obtained CFD results. This allowed for adequate resolution of the pressure variation without biasing the comparison. Figure 8 presents a closer look of the obtained surface pressures and compares the HMB solution with results from other partners as well. As can be seen, most CFD curves are within close proximity to the experimental data. Better agreement is obtained at the front of the fuselage and the agreement is still fair near the empennage and the fin of the model. The HMB solution is shown in pink colour and for the V1 station it appears to capture all features shown by the experiments. This is not the case for station S4 that is located near the rotor hub and just upstream of the exhausts. As can be seen, the CFD method tends to predict surface pressure coefficients above the values indicated by the experiments. The situation improves substantially for the station S7 that is located downstream in the rear fuselage. The discrepancies at station S4 for a particular set of azimuth angles (near 0 degrees) suggests that some vortex shedding from the hub may not be adequately resolved by the CFD. This is apparently due to the approximate hub geometry employed for computations and suggests that further work is needed in this area. Hub drag and the exact representation of hub geometry is

perhaps an area of research to be looked at in the near future. Figure 9 presents results for the blade loads for the economic cruise case. The first comparisons shown in Figure 9(a) show fair agreement between experiments and CFD near the front of the blade for azimuth angles of 90 and 270 degrees. For that figure the raw experimental data were phase averaged and used for comparisons. The discrepancies appear not to be present in Figure 9(a) where the experiments were processed removing fault or intermittently-working transducers and re-constraining the loads of one blade using the good, working transducers of all other blades. This was necessary in the GOAHEAD data due to a number of transducers failing or working intermittently during the test. The agreement between HMB and the processed data is now much better and this suggests that careful consideration of the outcome of the experiment is needed before comparing with CFD results. It is remarkable that overall, results contributed by several GOAHEAD partners show good agreement between codes and good agreement with experiments. The coarse resolution of the transducers doesn't allow for accurate chord-wise integrations though at all available stations along the chord, the agreement with the experiments is more than encouraging, given the complexity and difficulty of this flow.

The investigation of the main rotor-fuselage interactional aerodynamics for the 'intermediate' mesh showed that with the present method, this important aerodynamic effect was captured using the mesh with a total number of approximately $28 \cdot 10^6$ mesh points. As can be seen in Figure 5 the effect of the fuselage on the rotor loads is strong even at stations as outboards as 70% of the blade radius. The strong interaction leads to higher loads for the isolated rotor at the back of the disk and the opposite is the case for the front. Although this phenomenon is well-understood by design engineers, it is very rare to see quantitative results for such cases, due to the difficulty of computing the flow and the lack of appropriate test cases. The fidelity of the computations was ascertained by comparisons between the HMB results and the GOAHEAD experiments for the economic cruise.

4 Conclusions

The CFD results obtained for the GOAHEAD cases were all computed on an in-house Linux cluster and the HMB solver. The total time devoted to the rotor-body test case computations and was approximately one month. Improvements in the CFD method coupled with performance updates of the used Linux cluster compensated for the increased mesh sizes in the second phase of the computations. A comparison of the results obtained using the HMB method with experimental data for the GOAHEAD economic cruise test case shows that the method is capable of resolving the main aerodynamic flow features for the coarse blind test phase mesh, as well as, for the improved and refined post-wind tunnel test mesh. The improvements in mesh topology and the increase in mesh density clearly improved the spatial resolution of the flow. However, comparisons of the blind test phase and post-WT data with the experimental data, as well as, CFD results of the other GOAHEAD partners shows that the effect of the differences in employed rotor trim state and differences in the used geometry seems to be at least as significant as the improvements in the mesh topologies and sizes.

References

- [1] Y. Park, H.J. Nam, and O.J. Kwon. Simulation of unsteady rotor-fuselage aerodynamic interaction using unstructured adaptive meshes. American Helicopter Society 59th Annual Forum, Phoenix, Arizona, May 6-8., 2003.
- [2] Y. Park and O. Kwon. Simulation of unsteady rotor flow field using unstructured adaptive sliding meshes. J. American Helicopter Society, 49(4):391–400, 2004.
- [3] H.J. Nam, Y. Park, and O.J. Kwon. Simulation of unsteady rotor-fuselage aerodynamic interaction using unstructured adaptive meshes. J. American Helicopter Society, 51(2):141–148, 2006.
- [4] T. Renaud, C. Benoit, J.-C. Boniface, and P. Gardarein. Navier-stokes computations of a complete helicopter configuration accounting for main and tail rotor effects. 29th European Rotorcraft Forum, Friedrichshafen, Germany, September, 2003.
- [5] G. Barakos, R. Steijl, K. Badcock, and A. Brocklehurst. Development of CFD Capability for Full Helicopter Engineering Analysis. 31st European Rotorcraft Forum, 13-15 September 2005, Florence, Italy, 2005.
- [6] R. Steijl and G.N. Barakos. Sliding Mesh Algorithm for CFD Analysis of Helicopter Rotor-Fuselage Aerodynamics. *Int. J. Numer. Meth. Fluids*, 58:527–549, 2008.
- [7] R. Steijl and G.N. Barakos. Computational Study of Helicopter Rotor-Fuselage Aerodynamic Interactions. *AIAA Journal*, 47(9):2143–2157, 2009.
- [8] A.G. Brand, H.M. McMahon, and N.M. Komerath. Surface Pressure Measurements on a Body Subject to Vortex Wake Interaction. *AIAA journal*, 27(5), 1989.
- [9] J.M. Kim and N.M. Komerath. Summary of the interaction of a Rotor Wake with a Circular Cylinder. *AIAA journal*, 33(3), 1995.
- [10] C.E. Freeman and R.E. Mineck. Fuselage Surface Pressure Measurements of a Helicopter Wind-Tunnel Model with a 3.15-Meter Diameter Single Rotor. Technical Report TM-80051, NASA, 1979.
- [11] J.W. Elliott, S.L. Althoff, and R.H. Sailey. Inflow Measurements Made With a Laser Velocimeter on a Helicopter Model in Forward Flight - Volume I: Rectangular Planform Blades at an Advance Ratio of 0.15. Technical Report TM-100541, NASA, 1988.
- [12] J.W. Elliott, S.L. Althoff, and R.H. Sailey. Inflow Measurements Made With a Laser Velocimeter on a Helicopter Model in Forward Flight - Volume II: Rectangular Planform Blades at an Advance Ratio of 0.23. Technical Report TM-100541, NASA, 1988.
- [13] O. Boelens, G. Barakos, M. Biava, A. Brocklehurst, M. Costes, A. D’Alascio, M. Dietz, D. Drikakis, J. Ekatarinaris, I. Humby, W. Khier, B. Knutzen, F. Le Chuiton, K. Pahlke, T. Renaud, T. Schwarz, R. Steijl, L. Sudre, L. Vigevano, and B. Zhong. The Blind-Test Activity of the GOAHEAD Project. 33rd European Rotorcraft Forum, Kazan, Russia, September, 2007.
- [14] R. Steijl, G.N. Barakos, and K.J. Badcock. A Framework for CFD Analysis of Helicopter Rotors in Hover and Forward Flight. *Int. J. Numer. Meth. Fluids*, 51:819–847, 2006.
- [15] A. Jameson. Time Dependent Calculations Using Multigrid, with Applications to Unsteady Flows past Airfoils and Wings. AIAA Paper 1991-1596, 10th Computational Fluid Dynamics Conference, Honolulu, Hawaii, June 24-26, 1991.
- [16] A. Spentzos, G. Barakos, K. Badcock, B.E. Richards, P. Wernert, S. Schreck, and M. Raffel. CFD Investigation of 2D and 3D Dynamic Stall. *AIAA J.*, 34(5):1023–1033, 2005.

Acknowledgement

This work was supported by the European Union under the Integrating and Strengthening the European Research Area Programme of the 6th Framework, Contract Nr.516074 (GOAHEAD project). Some of the computations presented in this paper were carried out

using the Hector super-computer of the UK under the EPSRC grant EP/F005954/1.

it as part of their paper. The authors confirm that they give permission, or have obtained permission from the copyright holder of this paper, for the publication and distribution of this paper as part of the ICAS 2014 proceedings or as individual off-prints from the proceedings.

Copyright Statement

The authors confirm that they, and/or their company or organization, hold copyright on all of the original material included in this paper. The authors also confirm that they have obtained permission, from the copyright holder of any third party material included in this paper, to publish

Table 1: Meshes used in GOAHEAD project

	phase	blind	interm.	post-WT
fuselage:	blocks	1624	2298	2308
	cells	$6.5 \cdot 10^6$	$13.9 \cdot 10^6$	$14.0 \cdot 10^6$
main rotor:	blocks	856	1112	1112
	cells	$4.1 \cdot 10^6$	$11.1 \cdot 10^6$	$11.1 \cdot 10^6$
tail rotor:	blocks	-	376	376
	cells	-	$2.8 \cdot 10^6$	$2.8 \cdot 10^6$
total:	blocks	2480	3786	3796
	cells	$10.6 \cdot 10^6$	$27.8 \cdot 10^6$	$27.9 \cdot 10^6$

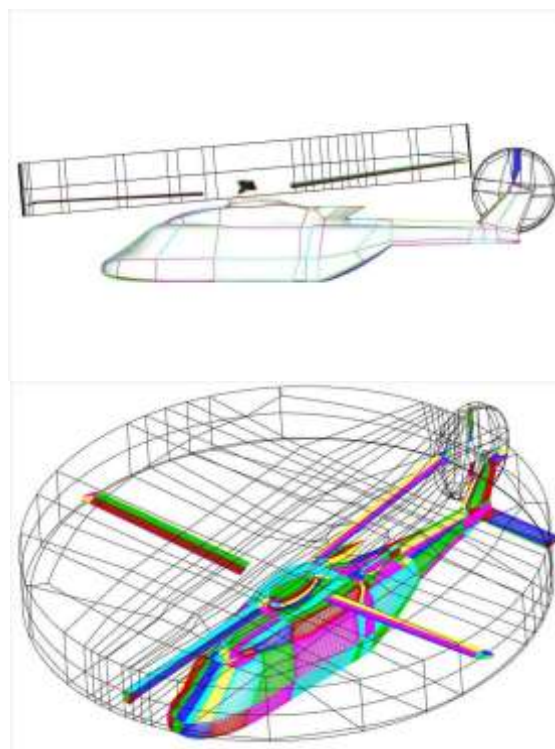


Fig. 1. Post-WT test phase. Full geometry modelled using a total of 6 sliding planes separating main rotor, tail rotor and fuselage meshes. For both rotors, 3 sliding planes form a 'drum' in which rotating rotor mesh is embedded in back ground fuselage mesh.

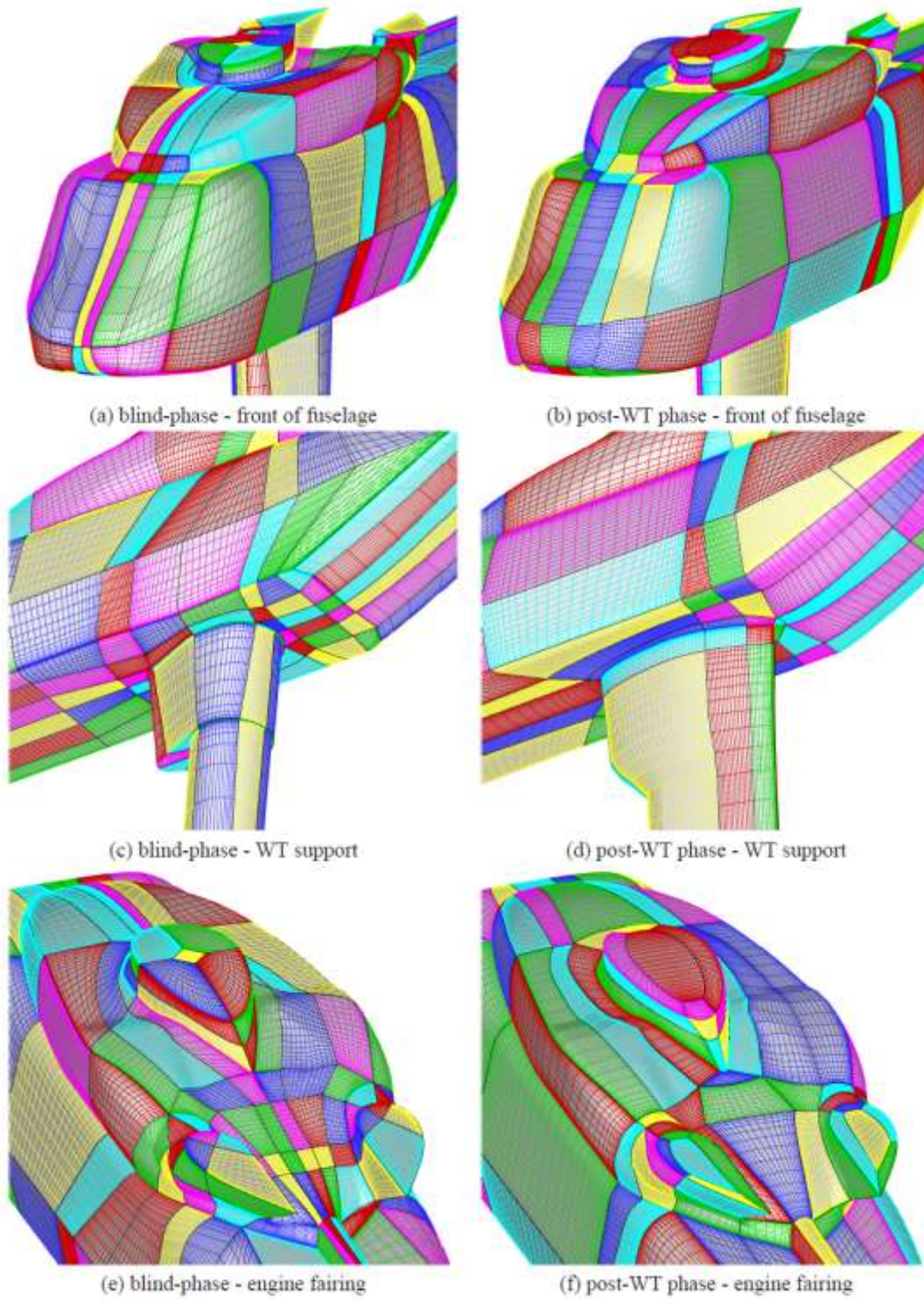
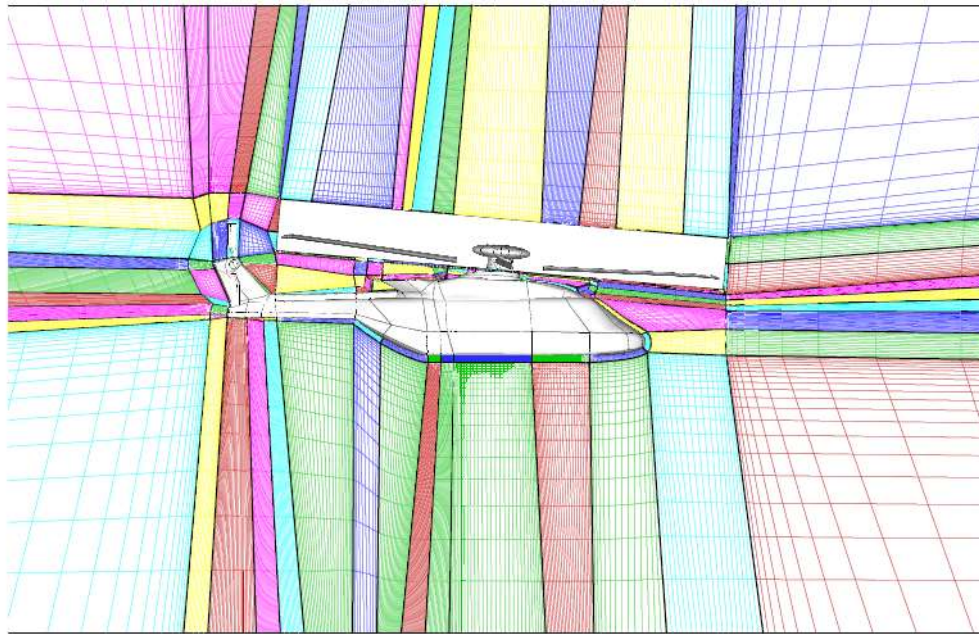
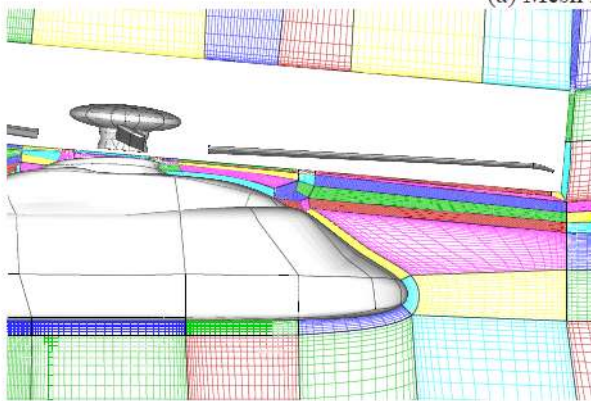


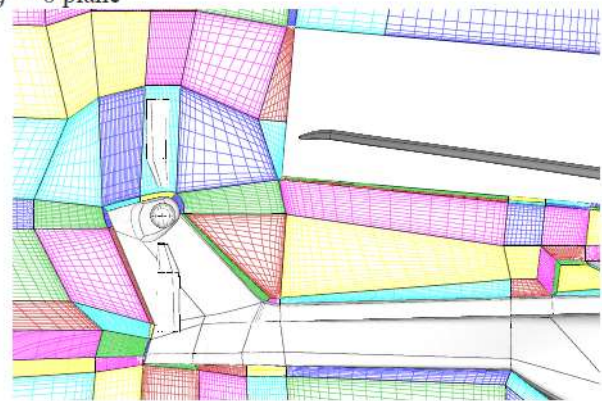
Fig. 2. Comparison of meshes used in the CFD simulations for the blind-phase and post-WT phase of the GOAHEAD project.



(a) Mesh in $y = 0$ plane

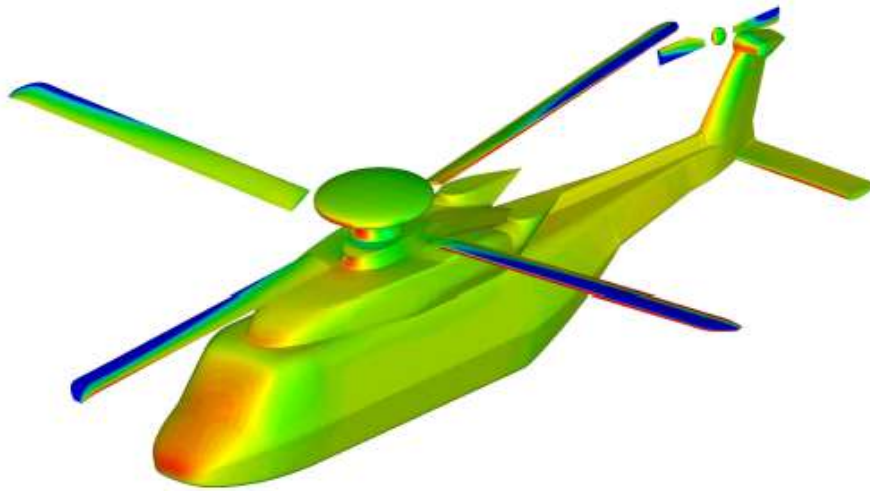


(b) Zoom of nose region of mesh in $y = 0$ plane

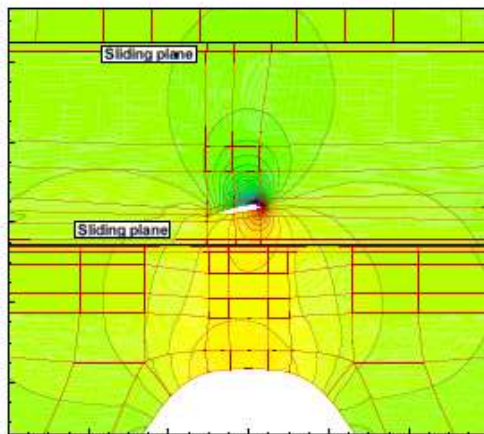


(c) Zoom of tail region of mesh in $y = 0$ plane

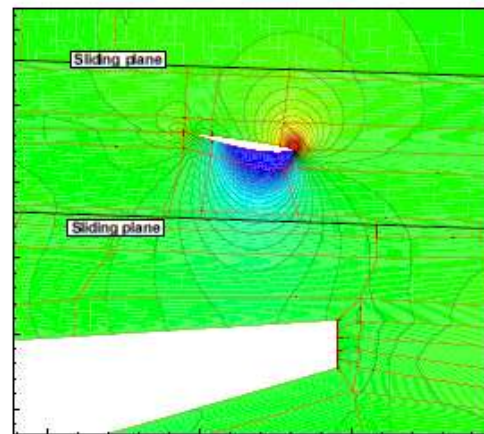
Fig. 3. GOAHEAD full helicopter geometry. The mesh in the $y = 0$ plane is shown, which does not constitute a symmetry plane. The rotor meshes are not shown for clarity. The mesh shown is the 'intermediate' mesh with WT support and has 3786 blocks and $27 \cdot 10^6$ cells. (a) global view of mesh, (b) detail of mesh in nose region, (c) close-up of mesh in tail region.



(a) Surface pressure coefficient at $\psi = 90^\circ$



(b) main rotor-fuselage interaction



(c) tail rotor-fin interaction

Fig4. GOAHEAD full helicopter geometry. Economic cruise condition. Instantaneous pressure coefficients are shown. (a) instantaneous surface pressure coefficient at main rotor azimuth of 90 degrees, (b) main rotor-fuselage interaction, $x = 0.75$ cross section (approx. mid span of blade), (c) tail rotor fin interaction, $z = 0.775$ cross-section, at base of fin.

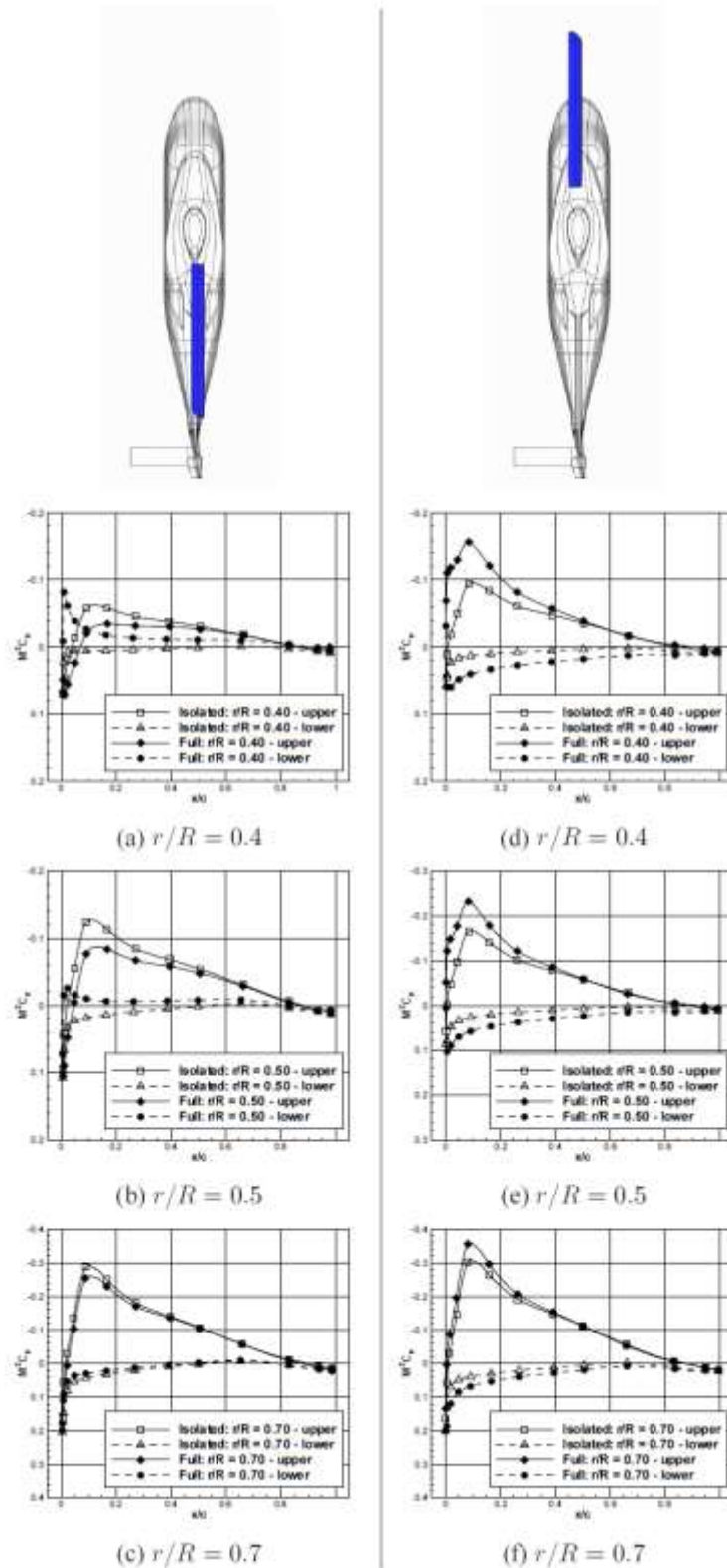


Fig 5. Effect of rotor-fuselage interaction on the blade loading for the GOAHEAD economic cruise test case. Sectional blade loading are compared for the full helicopter and an equivalent isolated rotor case.

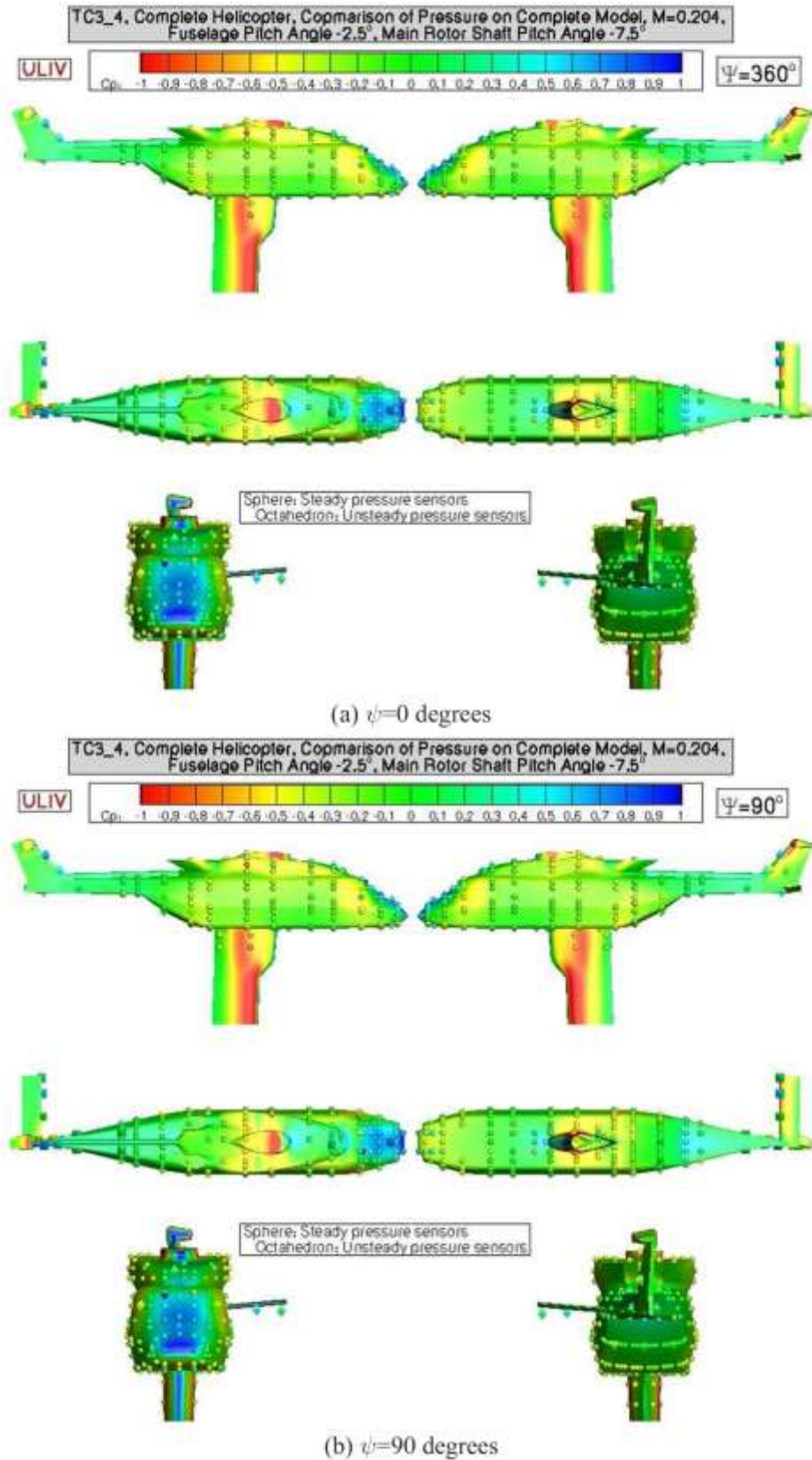


Fig 6. Comparison between CFD and experiments for the Economic Cruise (TC3-4) case. The spots on the fuselage correspond to the unsteady pressure transducers. Economic cruise conditions for the full helicopter configurations.

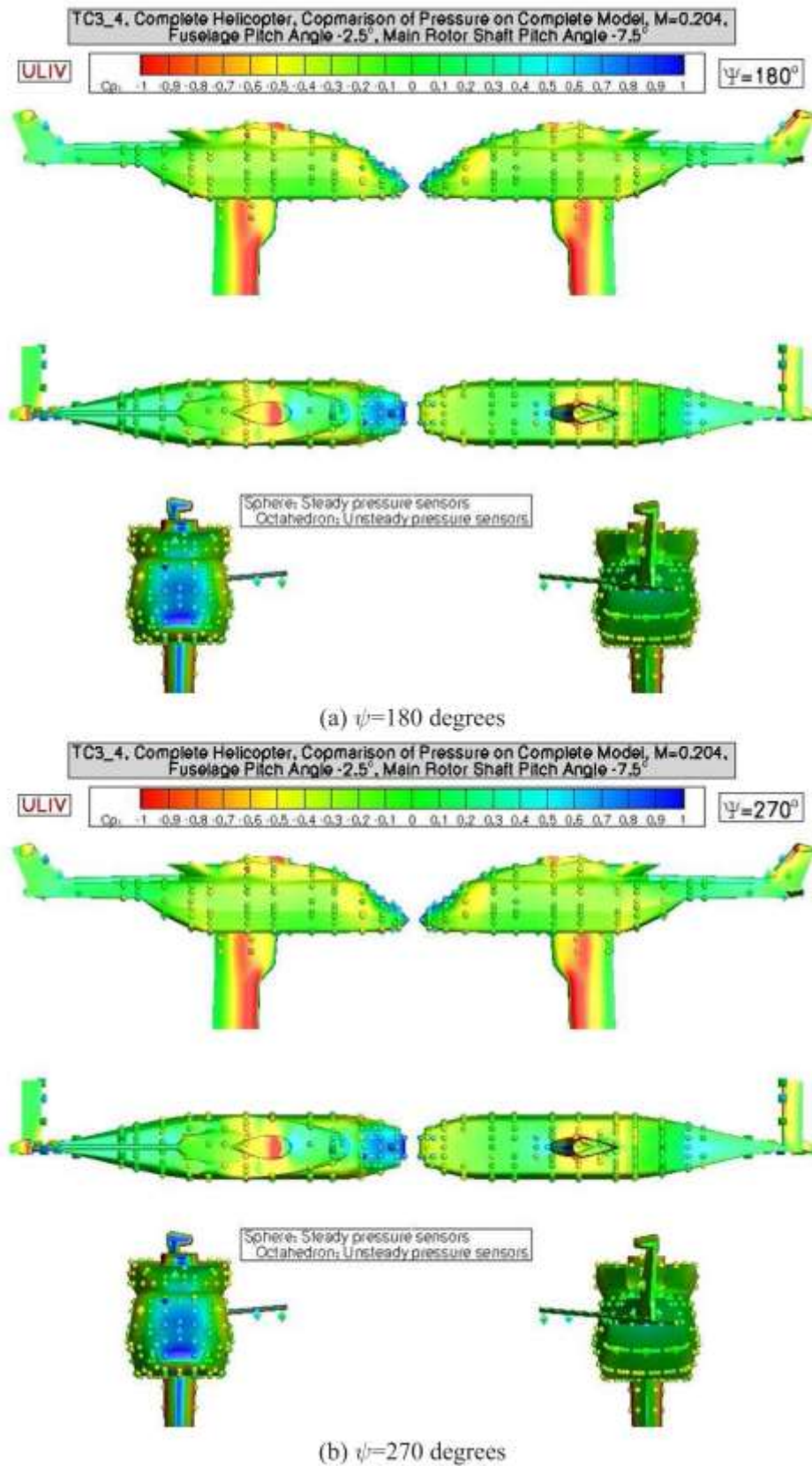
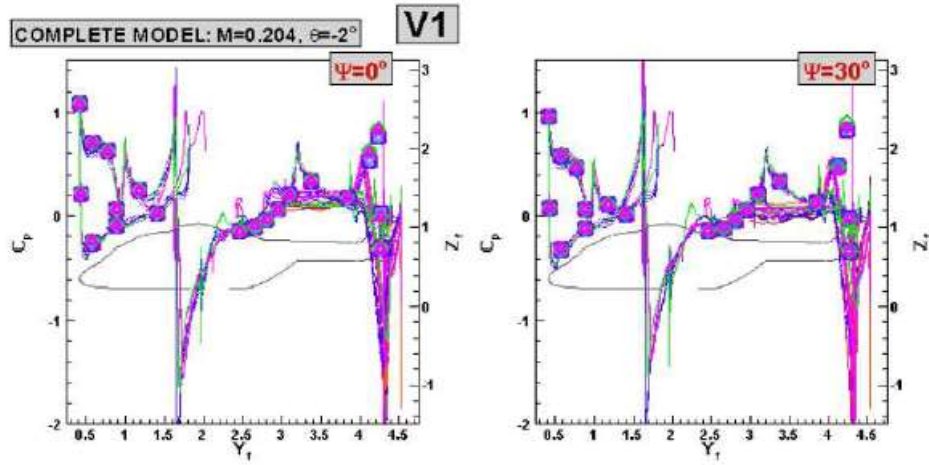
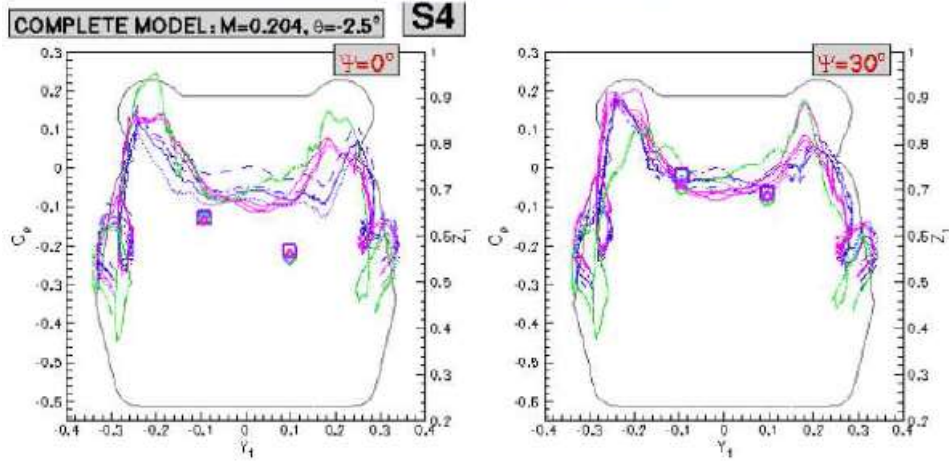


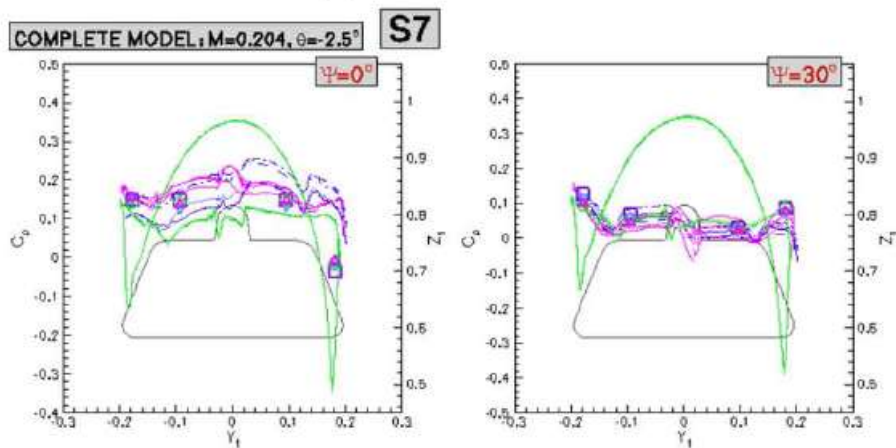
Fig 7. Comparison between CFD and experiments for the Economic Cruise (TC3-4) case. The spots on the fuselage correspond to the unsteady pressure transducers. Economic cruise conditions for the full helicopter configurations.



(a) Surface pressure along the fuselage



(b) Forward station S4



(c) Rearward station S7

Fig 8. Comparison between experiments and CFD for three stations along the fuselage for the Economic Cruise (TC3-4) case.

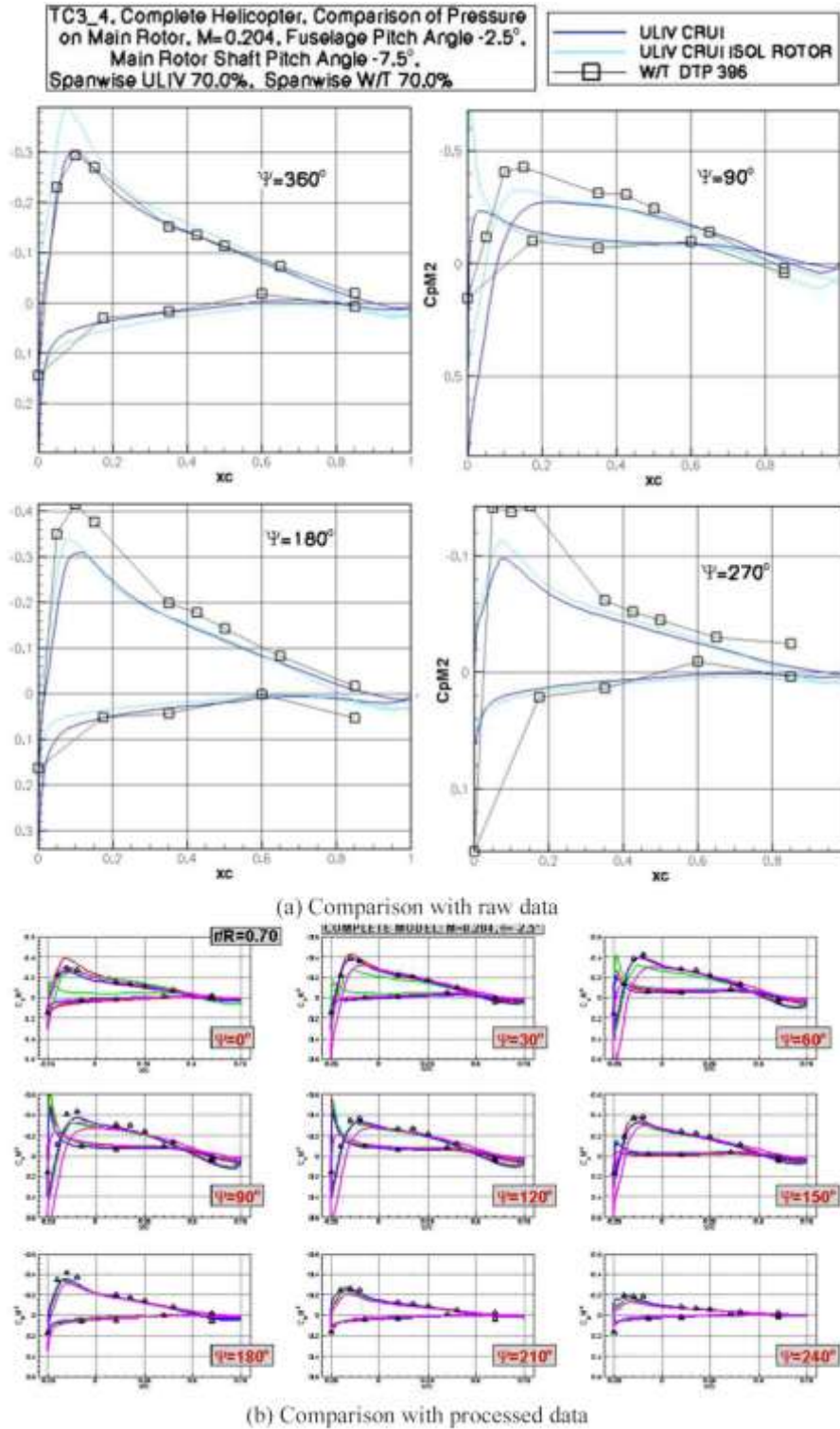


Fig 9. Comparison of sectional rotor loads between experiments and CFD for the Economic Cruise (TC3-4) case.